Article

Journal of Nanoscience and Nanotechnology
Vol. 15, 8790–8796, 2015
www.aspbs.com/jnn

All Ink-Jet Printed P3HT:PCBM Organic Solar Cells on ITO-Coated Glass Substrate

Eung-Kyu Park[1], Jae-Hyoung Kim[1], Dong-Hoon Lee[1], Kwang-Su Kim[2], Jin-Ha Kal[2], Jung Seok Hahn[2], and Yong-Sang Kim[1,∗]

[1] *School of Electronic and Electrical Engineering, Sungkyunkwan University, Suwon, 440-746, Korea*
[2] *Kolon Central Research Park, Kolon Research Institute, Yongin, 446-797, Korea*

Printed electronics have surfaced with a lot of interest recently. This paper reports development of a non vacuum process for fabricating poly(3-hexylthiophene):[6,6]-pheny-C_{61}-butyric acid methyl ester organic solar cells (OSCs) using ink-jet printing technique. The printing conditions of different layers were optimized to avoid the coffee ring effect and the Marangoni effect. The effect of substrate's temperature and drop spacing size was compared to obtain uniform layers. We controlled the substrate temperature ranging from 30 °C to 80 °C and varied the spacing size between two lines ranging from 10 μm to 80 μm during printing. The device characteristics were analyzed using alpha step and solar simulator. The optimized printed conditions for ZnO are 50 °C substrate temperature and 50 μm spacing size. For the active layer, PEDOT:PSS and Ag electrode, the optimized conditions are 50 °C/50 μm, 30 °C/30 μm and 80 °C/80 μm, respectively. The power conversion efficiency of the OSCs fabricated with optimized printing condition is 1.25%.

Keywords: Ink-Jet Printing, Organic Solar Cell, Solution Process, Nonvacuum Process.

1. INTRODUCTION

The organic solar cells (OSCs) are attracting a lot of attention as a renewable energy source owing to their advantages of easy fabrication, low-cost, light weight, solution process and the possibility to fabricate flexible devices.[1] Solution process signifies two advantages, which are, low temperature and no vacuum process.[2,3] The vacuum process includes evaporation, chemical vapor deposition (CVD), etc., which are expensive, complicated and inefficient.

Thin film deposition from solution at relatively low temperatures results in limited material usage and low fabrication cost of the organic solar cells.[4,5] These advantages open new market of solar cells, which seems impossible using other processes. However, there is inherently a large amount of waste in spin casting and it is not compatible with large processing area. In addition, while small devices are reproducible, techniques have not been developed that confirm the scalability of the technology.[6,7]

Printing technologies have attracted considerable attention for organic electronics due to their potentially high volume, low cost processing and improve selectivity. Printing technologies include screen printing,[8] gravure printing,[9] imprinting and ink-jet printing. Among several printing methods, ink-jet printing is a promising technique for electronics because of cost-efficient and precise processing.[10,11] Additionally, ink-jet printing can be used for patterning every material such as metal, semiconductor, and insulator. Special conducting inks are typically used for electronics, due to their chemical stability in ambient atmosphere and good electrical conductivity.

Ink-jet printing of layers faces two types of problems, Marangoni flow and coffee ring effect. When the electrodes are subjected to drying, the edges dries faster than the center and so the ink flow towards the edges. But due to surface tension, Marangoni flow occurs, which results in recirculation of the solvent in the droplet. This leads to the distortion in the morphology of electrode. In coffee ring effect, at low temperature, particle has enough time to move towards the edge. Therefore, the movement of particles results in uneven drying speed and distorts the electrode. Drop spacing affects the time of evaporation as the total volume of ink is increased or decreased.[12]

∗Author to whom correspondence should be addressed.

 1533-4880/2015/15/8790/007 doi:10.1166/jnn.2015.11523

A variety of published work focusses on non vacuum processed solar cells. However, reports on all ink-jet printed device and optimization of each layer is scarce. Few efforts have been made to fabricate ink jet-printed bulk-heterojunction solar cells. Brabec et al. recently reported the solar cell devices fabricated by inkjet-printing P3HT:PCBM formulated with various solvent mixtures on doctor-bladed PEDOT:PSS layer.[4, 13, 14] Aernouts et al. also reported the device performance of P3HT:PCBM active layer with high boiling point solvent mixtures for reducing coffee-ring effect.[6] Similarly, Bruno et al. used ink-jet printed P3HT:PCBM layer and optimized the morphology and mixture ratio of P3HT:PCBM.[15] Eom et al. reported bulk heterojunction polymer solar cells fabricated with an inkjet-printed poly(3,4-ethylenedioxythiophene):poly(styrenesulfonate) (PEDOT:PSS) layer. The morphology and electrical properties of the inkjet-printed PEDOT:PSS layer, as well as the overall device performance, was dramatically affected by the ink formulations containing additives, such as glycerol and a surfactant.[16, 17] In a related work, Jung et al. used all ink-jet printed PCDTBT:PCBM organic solar cell in a conventional structure, which focused on different solvent mixture ratio and reported a PCE of 4.85% and Hermerschmidt et al. used PCDTBT and Si-PCPDTBT as donor material and reported a PCE of 4.91% and 5.66%, respectively.[18, 19]

Therefore, in this study, we report the use of ink-jet printing and the optimized ink-jet printing conditions for the high performname OSCs. A range of substrate temperatures and drop spacing size were taken into consideration to print all the layers of OSCs. The electrical and optical properties of the devices were analyzed.

2. EXPERIMENTAL DETAILS

We fabricated an all solution processed organic solar cell using an ink-jet printer (Omijet100, UNIJET Co.). The printer employs a piezoelectric jetting head of 10 pL at a pulse wave form which applies a voltage of 20 V for 2 μs. The head jets 7.9 pL of ink at a velocity of 4.24 m/s through each nozzle at a frequency of about 1 kHz. Figure 1(a) explains the terms and inkjet printing mechanism used in this work. Figure 1(b) shows the schematic of organic solar cell with the structure of ITO/ZnO/P3HT:PCBM/PEDOT:PSS/Ag. For the fabrication, ITO glass substrates were cleaned in an ultrasonic bath with acetone, isopropyl alcohol, and deionized water for 20 min, respectively. Zinc oxide (ZnO) was used as a buffer layer for hole-blocking between the active layer and bottom electrode. ZnO solution was ink-jet printed onto ITO substrate and then annealed at 200 °C for 20 min in dry oven in ambient air condition. The ZnO solution was prepared by sol–gel method. The ZnO precursor, zinc acetate (Sigma-aldrich) and ethanolamine (Sigma-aldrich) was dissolved in the solution of 2-methoxyethanol at a concentration of 0.5 mol/L. The active layer (P3HT:PCBM) was deposited on ZnO layer by ink-jet printing and then thermally annealed at 120 °C for 10 min in a dry oven in ambient air. The P3HT:PCBM mixture (P3HT:PCBM = 1:1 weight ratio) was dissolved in chlorobenzene (40 mg/ml). In order to deposit hydrophilic PEDOT:PSS (Clevios PV P4083) solution on hydrophobic active layer, PEDOT:PSS was mixed with 0.5 vol% of Triton X-100 ($C_{14}H_{22}O(C_2H_4O)n$) non ionic surfactant. This solution was then spin coated on hexamethylene disilazane which was pre-coated on the active layer. Thermal pre-annealing was conducted at 160 °C for 10 min in a dry oven in ambient air. Ag top electrode (100 nm) was deposited on PEDOT:PSS layer by ink-jet printing and then dried at 120 °C for 10 min in a dry oven. The area of electrode was 0.1 cm^2. UV/visible spectrophotometer (Shimadzu UV-1601) was used to study light absorption of the various stacks of active layers. J–V characteristics were measured with J–V curve tracer (Eko MP-160) and solar simulator (Yss-E40, Yamashita Denso) under AM 1.5G (100 mW/cm^2) irradiation intensity. Entire fabrication and measurement processes were conducted in ambient air.

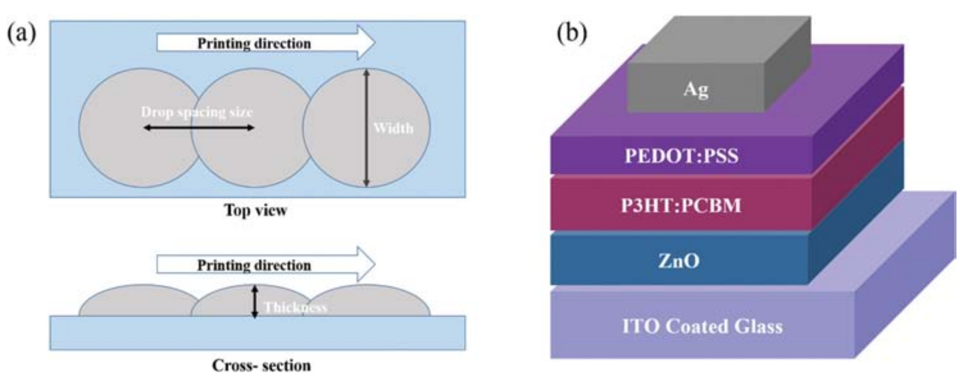

Figure 1. (a) Illustrations explaining drop width, drop spacing and layer thickness (b) the schematic of the inverted organic solar cell showing ITO/ZnO/P3HT:PCBM/PEDOT:PSS/Ag layers.

3. RESULTS AND DISCUSSION

Figure 2(a) shows the alpha step profile and optical microscope image of the printed ZnO. We controlled the substrate temperature ranging from 30 °C to 80 °C and varied the spacing size between two lines ranging from 10 μm to 80 μm during printing. Figure 2(b) shows the resulting thickness and width of ZnO layer with varied printing condition. At all temperature, the width of the ZnO layer exponentially decreased when the drop spacing size was increased. The surface of the ZnO layer became smoother when the temperature and spacing size decreased. Drop spacing and substrate temperature have an influence on total evaporation time and particle flow speed.[20] We settled to an optimized condition of 50 μm spacing size with a substrate temperature of 50 °C for ZnO layer printing to obtain the most smooth morphology of the layer. The coarse morphology of the layer consequence in poor contact between the active layer and ITO and increases the resistance.

Figure 3(a) shows the optimization of printing condition for the active layer. We printed the active layer on the printed ZnO layer. The substrate temperature was varied

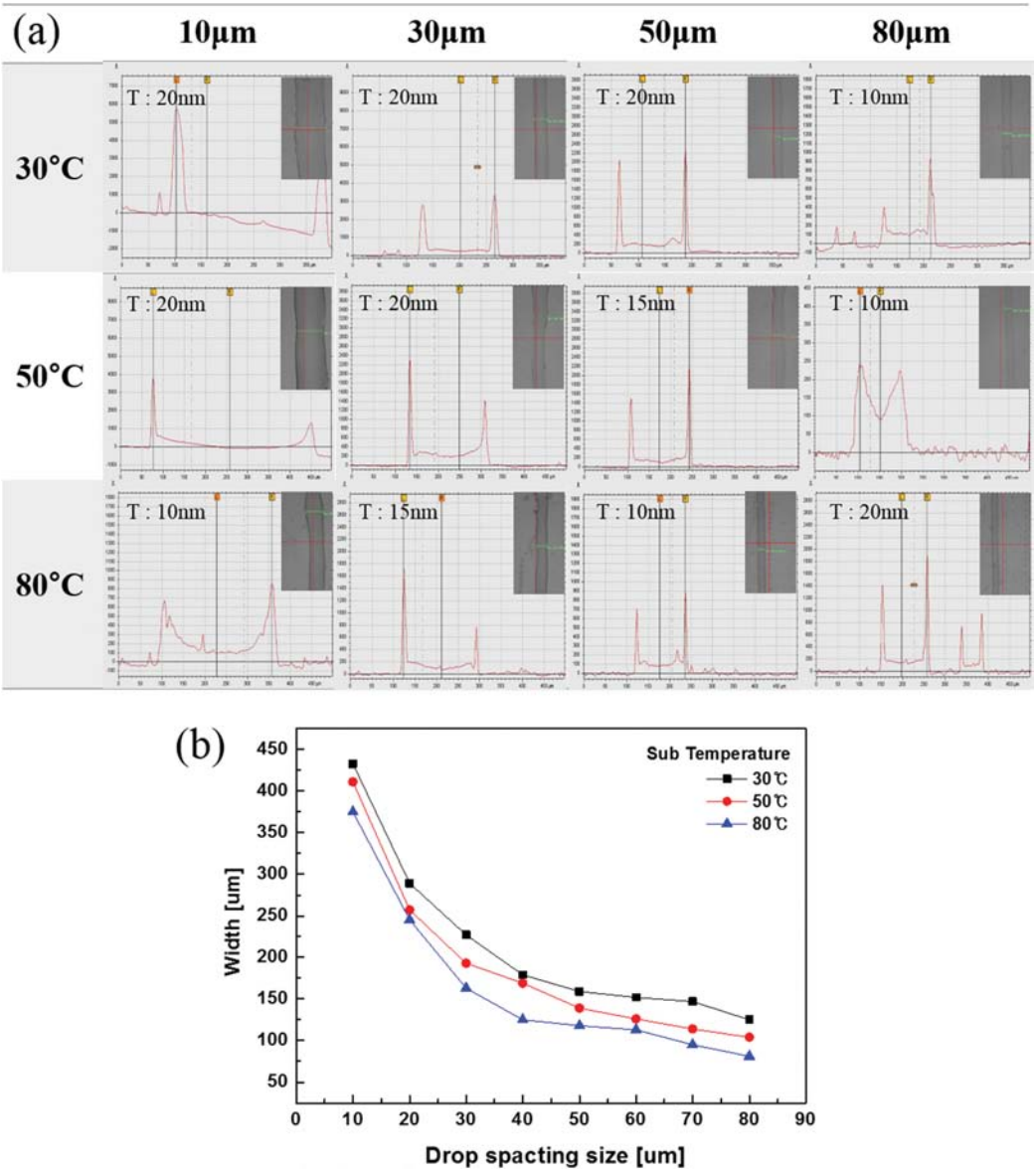

Figure 2. Ink-Jet printed ZnO layer (a) optical microscope image and alpha step profile of the layer (T = Thickness); (b) width of the printed ZnO layer as a function of substrate temperature and spacing size, -■-: 30 °C, -●-: 50 °C, -▲-: 80 °C. Optimized condition: spacing 50 μm and temperature 50 °C.

between 30 °C and 80 °C and the spacing size ranged from 50 μm to 150 μm during printing. P3HT:PCBM followed the same mechanism as that of ZnO and so same condition, 50 °C substrate temperature with 50 μm spacing size was opted for printing. Figure 3(b) shows the light absorption of multiple stacks of printed active layer. Layer by layer, we printed stacks of P3HT:PCBM to increase the light absorption. The main absorption wavelength region of PCBM is 330 nm and for P3HT is from 400 nm to 600 nm. The black line (Solid Square) represents the absorption of control device fabricated using spin coating. The increased thickness of active layer improved the light absorption of the device and hence the charge separation and power conversion efficiency.[21]

Table I. Performance of spin coated and ink-jet printed organic solar cells with multiple active layer stacking.

	J_{sc} [mA/cm^2]	V_{oc} [V]	F.F	PCE [%]
Control	10.90	0.60	0.48	3.12
1-stack	6.21	0.59	0.38	1.41
2-stack	8.50	0.60	0.45	2.35
3-stack	7.19	0.60	0.39	1.73

The measured J–V characteristics of spin coated organic solar cells and cells with ink-jet printed active layer (with multiple stacking) using a solar simulator under AM 1.5G (100 mW/cm^2) irradiation intensity is shown in Figure 3(c). In this device, only the active layer was

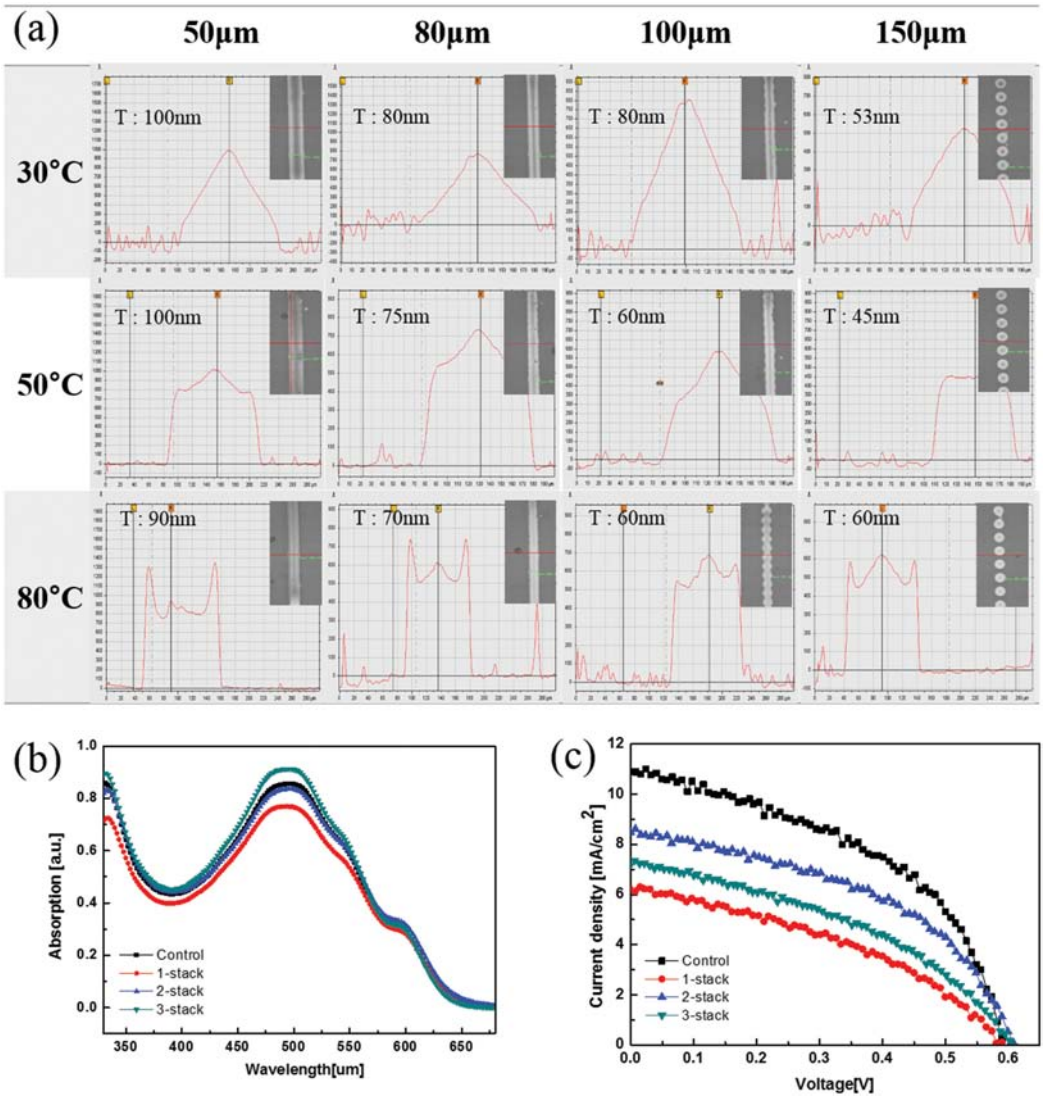

Figure 3. Ink-Jet printed active layer (a) optical microscope image and alpha step profile of the layer (T = Thickness), optimized condition: spacing 50 μm and temperature 50 °C; (b) UV-Visible absorption spectra of ITO/P3HT:PCBM layer; (c) J–V characteristics of control device and devices with printed active layer. (-■-: control, -●-: 1 stack, -▲-: 2 stack, -▼-: 3 stack).

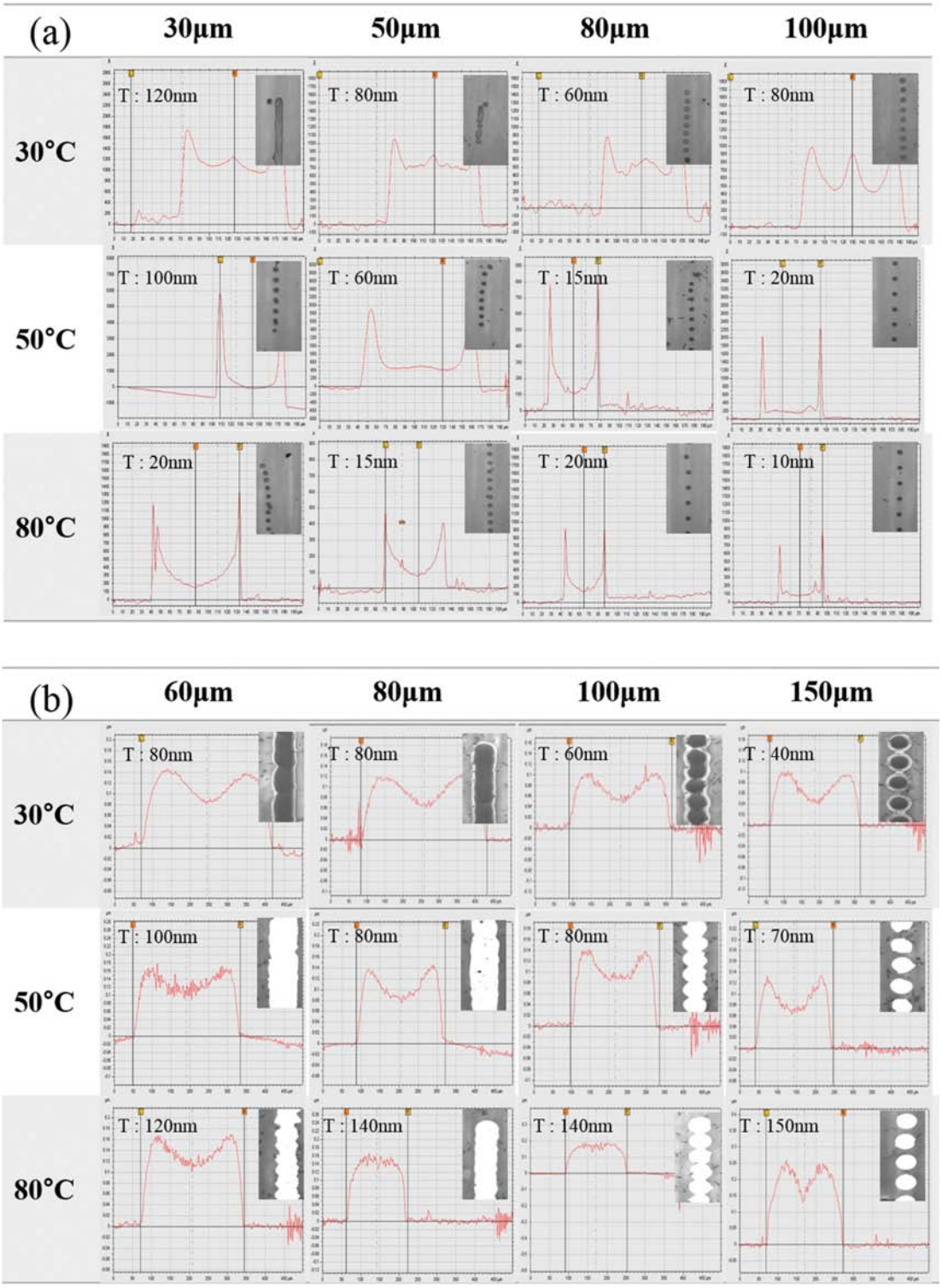

Figure 4. (a) Optical microscope image and alpha step profile of printed PEDOT:PSS layer (T = Thickness), optimized condition: spacing 30 μm and temperature 30 °C; (b) optical microscope image and alpha step profile of printed Ag electrode (T = Thickness), optimized condition: spacing 80 μm and temperature 80 °C.

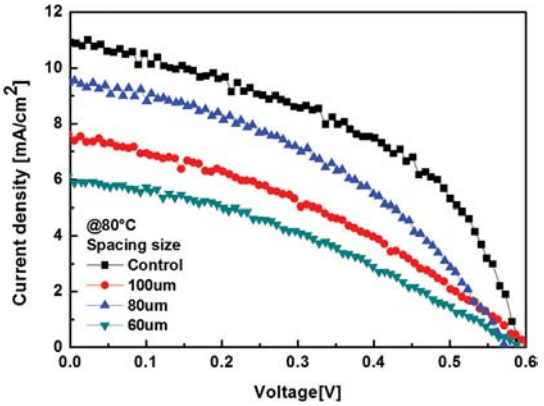

Figure 5. *J–V* characteristic of control device and devices with printed Ag electrode, -■-: control, -●-: 100 μm, -▲-: 80 μm, -▼-: 60 μm.

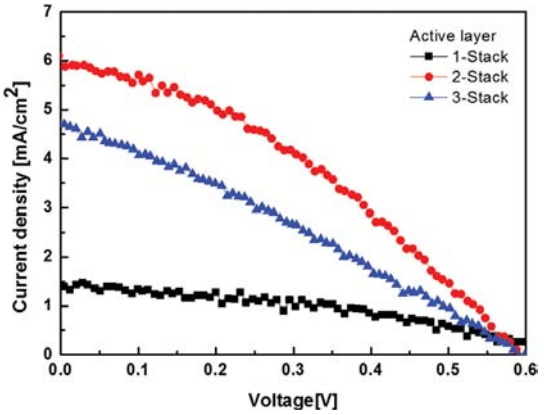

Figure 6. *J–V* characteristics of all ink-jet printed inverted organic solar cells with different stacks of active layer; -■-: 1 stack, -●-: 2 stack, -▲-: 3 stack.

printed while the rest of the layers were processed conventionally. The control device (spin coating) showed a short circuit current density (J_{sc}) of 10.90 mA/cm^2. The ink-jet printed device with 1, 2, and 3 layers of P3HT:PCBM showed a J_{SC} of 6.21, 8.50 and 7.19 mA/cm^2, respectively. In most of the reported work, the thickness of the active layer is above 80 nm.[21, 22] The 3 layer stacked device showed lower J_{sc} even though it had higher absorption (Fig. 3(b)). The reason behind this can be attributed to the increased thickness of active layer. The high thickness increased absorption and also charge recombination, which decreased the performance of OSCs. The performances of solar cells with different number of active layer stacking are summarized in Table I.

Figure 4(a) shows the optimization of PEDOT:PSS printing condition. For PEDOT:PSS, the substrate temperature ranged from 30 °C to 80 °C and the spacing size between two lines ranged from 30 μm to 100 μm. Due to the difference in surface properties of PEDOT:PSS and other materials, the printing of PEDOT:PSS on the substrate with temperature above 30 °C and the spacing size above 30 μm was not successful.[23, 24] We also printed Ag electrode on PEDOT:PSS layer using ink-jet printer. Figure 4(b) shows the optimization of Ag electrode printing condition. For Ag electrode, the substrate temperature ranged from 30 °C to 80 °C and spacing sizes between two lines ranged from 60 μm to 150 μm. The measured *J–V* characteristics of vacuum processed organic solar cells and cells with ink-jet printed Ag electrode (at 80 °C and different spacing size of Ag electrode) using solar simulator is shown in Figure 5. Here, only the Ag electrode was printed while the rest of the layers were processed conventionally. The control device showed a J_{sc} of 10.90 mA/cm^2. The ink-jet printed device with Ag electrode of spacing size 60, 80 and 100 μm showed a J_{sc} of 6.02, 9.49 and 7.55 mA/cm^2, respectively. The device with a spacing size of 80 μm (80 °C) demonstrated almost similar performance as that of control device. The ink-jet printed devices showed lower F.F and J_{sc} because of the increase in series resistance at the edge of electrode. The performances of solar cells with different spacing size of Ag electrodes are summarized in Table II.

Table II. Performance of vacuum processed and ink-jet printed organic solar cells with different spacing size of Ag electrode.

	J_{sc} [mA/cm^2]	V_{oc} [V]	F.F	PCE [%]
Control	10.90	0.60	0.48	3.12
100 μm	7.55	0.60	0.35	1.61
80 μm	9.49	0.57	0.41	2.24
60 μm	6.02	0.59	0.35	1.25

Table III. Performance of all ink-jet printed P3HT:PCBM organic solar cells with multiple active layer stacking.

	J_{sc} [mA/cm^2]	V_{oc} [V]	F.F	PCE [%]
1-stack	1.43	0.62	0.36	0.35
2-stack	6.02	0.60	0.35	1.25
3-stack	4.72	0.59	0.28	0.79

The measured *J–V* characteristics of all ink-jet printed (optimized condition) organic solar cells is shown in Figure 6. Based on the results, 50 °C/50 μm for ZnO, 50 °C/50 μm for P3HT:PCBM, 30 °C/30 μm for PEDOT:PSS and 80 °C/80 μm for Ag electrode was adjudged as the optimum printing condition. The all ink-jet printed device with 1, 2 and 3 stacks of active layer showed a J_{sc} of 1.43, 6.02 and 4.72 mA/cm^2, respectively. The performances of the solar cells are summarized in Table III.

4. CONCLUSION

We investigated the optimization of ink-jet printing condition for the fabrication of organic solar cells. Each layer of OSC was printed with varied substrate temperature and line spacing size; and their performance was

compared. The optimized printed conditions for ZnO are 50 °C substrate temperature with 50 μm spacing size. For P3HT:PCBM, PEDOT:PSS and Ag electrode, the conditions are 50 °C/50 μm, 30 °C/30 μm and 80 °C/80 μm respectively. The power conversion efficiency of ink-jet printed OSC with the optimized condition is 1.25%. A further detailed study to fabricate an ink-jet printed flexible based OSC and its application would increase the dimension of this research.

Acknowledgments: This work was supported by the Human Resources Development program (No. 20124010203280) of the Korea Institute of Energy Technology Evaluation and Planning (KETEP) grant funded by the Korea government Ministry of Trade, Industry and Energy.

References and Notes

1. H. Sirringhaus, T. Kawase, R. H. Friend, T. Shimoda, M. Inbasekaran, W. Wu, and E. P. Woo, *Science* 290, 2133 (**2000**).
2. D. Soltman and V. Subramanian, *Langmuir* 24, 2224 (**2008**).
3. M. Y. Lee, M. W. Lee, J. S. Park, and C. K. Song, *Microelectron. Eng.* 87, 2577 (**2010**).
4. C. N. Hoth, S. A. Choulis, P. Schilinsky, and C. J. Brabec, *Adv. Mater.* 19, 3973 (**2007**).
5. V. Marin, E. Holder, M. M. Wienk, E. Tekin. D. Kozodaev, and U. Schubert, *Macromol Rapid Comm.* 26, 319 (**2005**).
6. T. Aernouts, T. Alekandrov, C. Girotto, J. Genoe, and J. Poortmans, *Appl. Phys. Lett.* 92, 033306 (**2008**).
7. M. Al-Ibrahim, H. K. Roth, and S. Sensfuss, *Appl. Phys. Lett.* 85, 1481 (**2004**).
8. S. E. Shaheen, R. Radspinner, N. Peyhambarian, and G. E. Jabbour, *Appl. Phys. Lett.* 79, 18 (**2005**).
9. M. M. Voigt, R. C. I. Mackenzie, S. P. King, C. P. Yau, P. Atienzar, J. Dane, P. E. Keivanidis, I. Zadrazil, D. D. C. Bradley, and J. Nelson, *Sol. Energ. Mat. Sol. C* 105, 77 (**2012**).
10. S. H. Ko, H. Pan, C. P. Grigoropoulos, C. K. Luscombe, J. M. J. Frechet, and D. Poulikakos, *Nanotechonolgy* 18, 345202 (**2007**).
11. D. Kim, S. H. Lee, S. Jeong, and J. Moon, *Electrochem. SolidSt.* 12, H195 (**2009**).
12. D. H. Lee, K. T. Lim, E. K. Park, J. M. Kim, and Y. S. Kim, *Microelectron. Eng.* 111, 242 (**2013**).
13. C. N. Hoth, P. Schilinsky, S. A. Choulis, and C. J. Brabec, *Nano Lett.* 8, 2806 (**2008**).
14. C. N. Hoth, S. A. Choulis, P. Schilinsky, and C. J. Brabec, *J. Mater, Chem.* 19, 5398 (**2009**).
15. A. Bruno, F. Villani, I. A. Grimaldi, F. Loffredo, P. Morvillo, R. Diana, S. Haque, and C. Minarini, *Thin Solid Films* 560, 14 (**2014**).
16. S. H. Eom, H. Park, S. H. Mujawar, S. C. Yoon, S. S Kim, S. I. Na, S. J. Kang, D. Khim, D. Y. Kim, and S. H. Lee, *Org. Electron.* 11, 1516 (**2010**).
17. S. H. Eom, S. Senthiarasua, P. Uthirakumar, S. C. Yoon, J. Lim, C. Lee, H. S. Lim, J. Lee, and S. H. Lee, *Org. Electron.* 10, 536 (**2009**).
18. S. Jung, A. Sou, K. Banger, D. H. Ko, P. C. Y. Chow, C. R. McNeill, and H. Sirringhaus, *Adv. Funct. Mater.* 4, 1400432 (**2014**).
19. F. Hermerschmidt, P. Papagiorgis, A. Savva, C. Christodoulou, G. Itskos, and S. A. Choulis, *Sol. Energ. Mat. Sol. C* 130, 474 (**2014**).
20. J. H. Park and J. H. Moon, *Langmuir* 22, 3506 (**2006**).
21. Y. M. Nam, J. Huh, and W. H. Jo, *Sol. Energ. Mat. Sol. C* 94, 1116 (**2010**).
22. G. Li, V. Shrotriya, Y. Yao, and Y. Yang, *J. Appl. Phys.* 98, 043704 (**2005**).
23. A. W. Hains, J. Liu, A. B. F. Martinson, M. D. Irwin, and T. J. Mark, *Adv. Funct. Mater.* 20, 595 (**2010**).
24. Y. H. Kim, C. Sachse, M. L. Machala, C. May, L. Muller-Meskamp, and K. Leo, *Adv. Funct. Mater.* 21, 1076 (**2011**).

Received: 1 August 2014. Accepted: 1 December 2014.